Photomask image enhancement using grating-generated surface waves

Neal V. Lafferty,[a] Anatoly Bourov, Andrew Estroff, and Bruce W. Smith
Microsystems Engineering, College of Engineering, Rochester Institute of Technology, 82 Lomb Memorial Dr., Rochester, New York 14623, USA

(Received 27 June 2008; accepted 22 September 2008; published 1 December 2008)

In recent years, the anomalous transmission of subwavelength apertures has become an emergent subject within the physical sciences. While the gain mechanism of these structures is still uncertain, the effect has been observed in several studies. Similar transmission enhancements may be realized for near-wavelength sized photomask structures by including buried grooves in a dual write mask design. Several configurations of one-dimensional transmitting apertures and buried grooves have been investigated under TM illumination using the finite element method. Periodic subwavelength apertures with identical sized nontransmitting assist grooves were used to validate the model against reference data in the near-IR. The method was also used to investigate similar structures featuring a larger than wavelength transmitting aperture. Although transmission through the slot was increased by 1.67×, the primary lithographic benefit was an increase in the magnitude of the primary imaging orders relative to the zeroth diffracted order. A similar approach was extended to structures scaled to 248 nm to show application as a potential lithographic assist feature. A 5.7× transmission increase was observed using aluminum on fused silica configuration using 30 nm slots on a 192 nm pitch. © *2008 American Vacuum Society.* [DOI: 10.1116/1.3002560]

I. INTRODUCTION

As a primary driver of industry standards, optical lithography is constantly being pushed to its resolution limits. The typical parameters manipulated to achieve high resolution include the illumination wavelength (λ), numerical aperture, partial coherence (σ), and more recently the refractive index (n_i) of the image media.[1] Alternative resolution enhancement methods are continually sought, including approaches incorporated at the photomask. Periodic arrays of subwavelength slots in a photomask can lead to enhanced transmission properties depending on pattern layout, polarization, wavelength, and material properties.[2,3] Designs using buried grooves, referred to here as evanescent wave assist features, have revealed both near and far field benefits, including increased intensity and contrast enhancement of an aerial image.[4] These features function differently than traditional subresolution assist features, having the ability to increase the magnitudes of primary diffraction orders, not just reduce them.[5] Previous investigations with buried dielectric gratings and TM illumination have also shown aerial image enhancement; however, solutions have failed to converge for highly conductive materials. A study of the potential enhancement characteristics of metallics under TM illumination with and without slots is therefore desired. To that end, we have created a model using a finite element method (FEM) solver that can simulate these types of patterns.[6] The model uses a scattered harmonic analysis formulation and TM polarized incoming radiation in conjunction with perfectly matched layers and periodic boundary conditions.[6] Electromagnetic phenomena are easily observable by plotting any number of calculated variables together. Specifically, the modulation of power transmitted through an aperture and the role of surface plasmon polaritons in this process is of interest.

By incorporating buried groove structures parallel to a slot or contact, the relative magnitudes of the diffracted orders may be adjusted, resulting in aerial images with increased contrast.[3]

A. Surface plasmon polaritons

Surface plasmon polaritons, or SPPs, are local oscillations in the electron distribution at the surface of a material caused by an impinging electric field.[7] Conditions for the existence of SPPs are TM polarization and an interface between dielectric and conductive media.[7] In this case, the criterion for conductivity is the dielectric function (ε) where $\mathrm{Re}[\varepsilon]<0$. For a metal, this condition is satisfied below its plasma frequency (ω_p). Additionally, the incoming wave must couple from the surrounding environment to the metal surface, which can be accomplished through grating coupling.

Such a grating is engineered with a specific pitch (d) to allow an incoming wave with wavelength to diffract into orders specified by integer (m) having an angular spread, (θ) for a plane wave normally incident on an interface,

$$\sin\theta_m = m\frac{\lambda}{nd}. \tag{1}$$

In the limit, when d is equal to or less than λ/n, all orders are diffracted along the surface of the interface, resulting in evanescent orders.[8] Additionally, at pitches larger than λ, higher diffraction orders will still be evanescent. In the grating coupler application, this converts a normally incident wave of wave vector k to a wave with an in-plane wave vector, k_x. When k_x matches the propagation constant of the

[a]Electronic mail: nxl7930@rit.edu

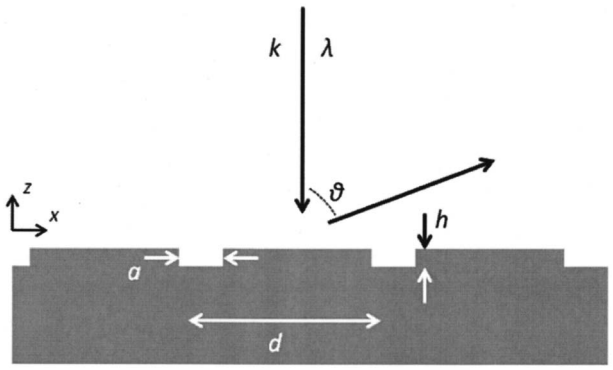

FIG. 1. Schematic of a grating structure used to diffract incoming radiation into surface waves. Relevant design parameters are labeled in the figure.

SPP, β, the phase match condition is satisfied and SPPs may be excited. Figure 1 describes the grating coupler geometry used in these experiments.

II. SLIT TRANSMISSION MODULATION

A. Subwavelength slit

In order validate the utility of the model, the well-studied case of transmission enhancement through a subwavelength slit surrounded by a variable number of grooves was used. The geometry and conditions studied were similar to those used by Lezec and Thio[2] and can be seen schematically in Fig. 2(a). Although originally studied as a single isolated slot, when periodic this type of feature is similar to a mask pattern. A freestanding silver film 340 nm thick with 100 nm wide grooves was investigated through wavelength from 630 to 770 nm under TM polarization. A central, fully transmitting groove was surrounded by a varying number of 50 nm grooves etched in the top surface of the conductor. The transmission enhancement was evaluated by integrating the time average power flow through the bottom of the simulation domain. Figure 3 illustrates a generic domain, with the left and right boundaries as periodic. The gradient regions at the top and bottom are perfectly matched layers to prevent reflections. Geometries at identical transmitting slot pitches without partially etched grooves (or assists) were also simulated and used to normalize the power flow data, yielding the power enhancement factor provided by the grooves. The results of this investigation can be seen in Fig. 4. In general, the model agrees with prior experiment, with a maximum of 1.7× enhancement seen in both cases at a wavelength near 720 nm. Interestingly, the peak power through the slot occurs at a wavelength slightly higher than the optimal wavelength for SPPs, which in this case is 650 nm.[2] The enhancement indicates that the method is capable of detecting influences caused by the surface patterned assist slots.

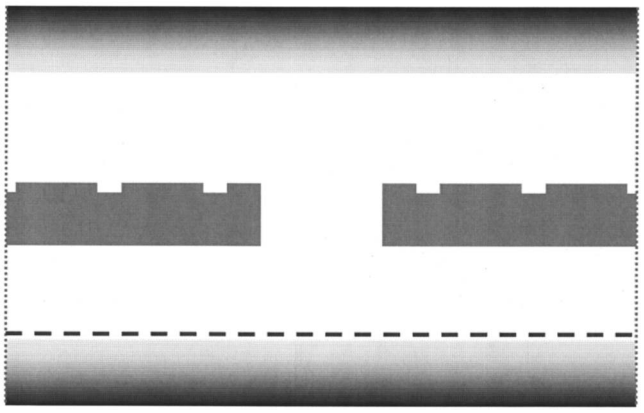

FIG. 3. FEM domain layout. The domain features periodic boundary conditions at both vertical bounds (dotted), and perfectly matched layers at the top and bottom (shaded) to eliminate unwanted reflections back into the system. The time average power output is determined by integrating the output power just above the bottom PML (dashed) across the domain.

B. Superwavelength slit

Although the case of the extreme subwavelength slit is an interesting physical phenomenon, lithographic features will generally be on order of the illuminating wavelength, if not larger, since they must generate diffraction orders for a pro-

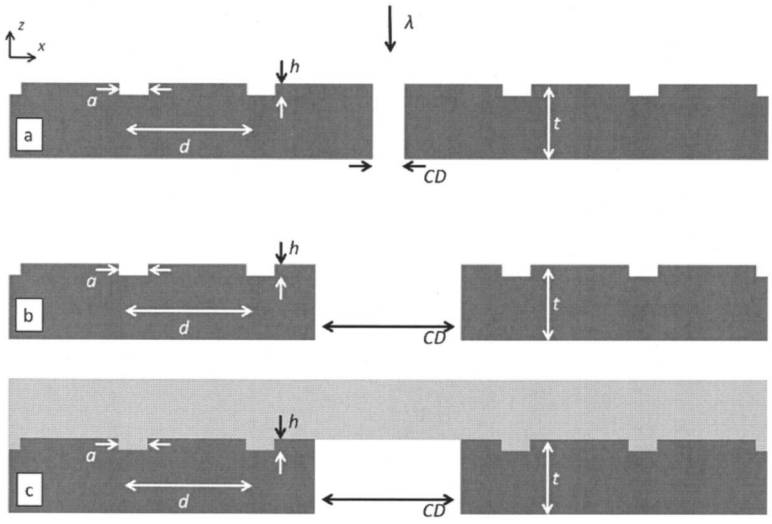

FIG. 2. Transmitting slot and assist groove layout for each of the slot-size regimes. The number of surrounding slits varies depending on case. (A) Freestanding subwavelength slot. (B) Freestanding superlambda slot. (C) Superwavelength slot bounded by fused silica. For all three cases, the transmitting slot and assist grooves have the same center to center distances.

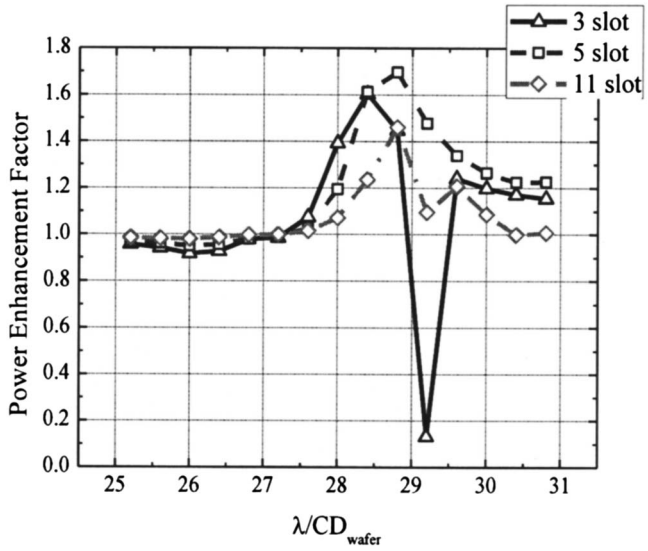

FIG. 4. Subwavelength (100 nm) main groove showing power enhancement with assist grooves vs identical unassisted cases. Both enhancement and suppression can be observed in this case, especially for the three and five slot cases. Best observed enhancement occurs near 720 nm.

jection lens to collect. Therefore the subwavelength transmitting slot was enlarged to 900 nm to approach a lithographic type feature, as in Fig. 2(b). The pitch of the main features and the surrounding assist grooves was kept identical to the subwavelength slot case. For a 4× reduction system, this slot width corresponds to a 320 nm feature on mask (80 nm on wafer) imaged with a KrF scanner, or a 248 nm feature on mask (62 nm on wafer) imaged with an ArF scanner. The results can be found in Fig. 5. In this case, the power enhancement through the system due to the assist grooves was again measured, with a peak of about 1.67× at 730 nm. The electric field just above the start of the perfectly matched layer (PML) was taken for the five assist slot case and its corresponding unassisted case. The Fourier transforms of both fields were compared to determine the assist feature's effect, if any, on the diffraction orders. Although in the assisted case, the zeroth order is increased slightly compared to the reference condition, the first and second orders show a larger relative increase which is beneficial for improving the

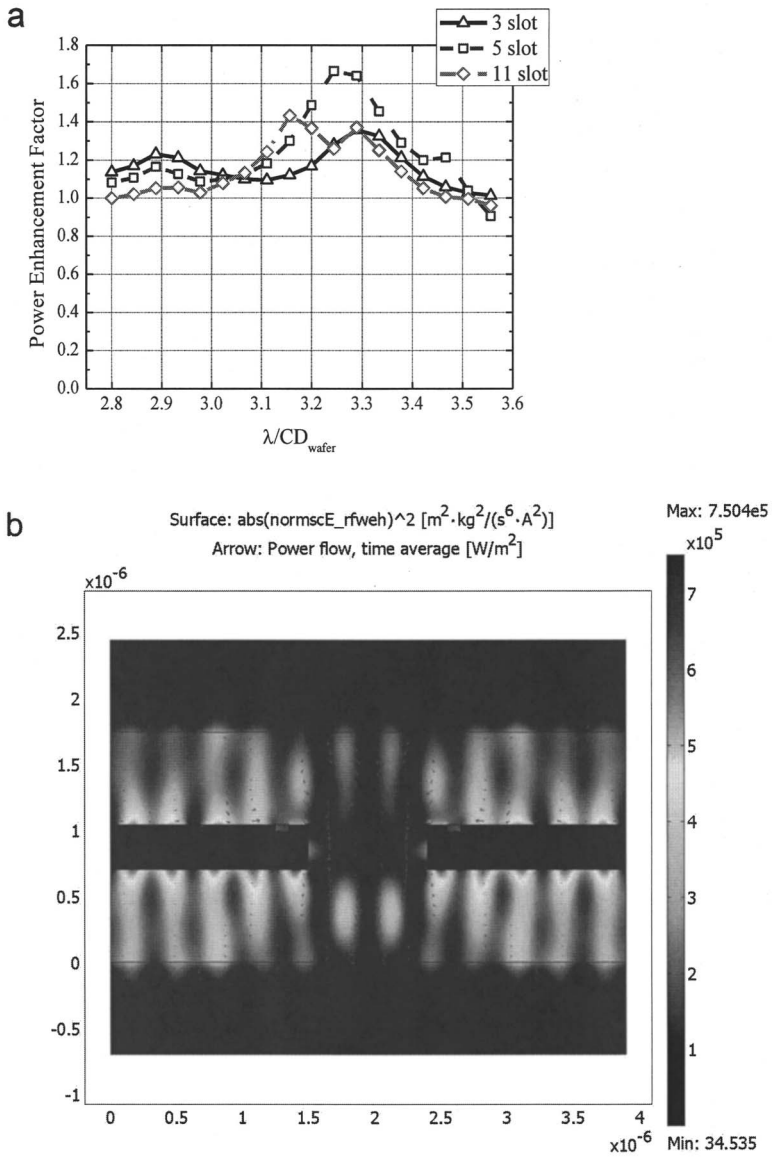

FIG. 5. (a) Superwavelength (900 nm) main groove showing power enhancement with assist grooves vs identical unassisted cases. In this case, best observed enhancement occurs near 730 nm. (b) Surface plot overlaid with cross section of the domain. The surface shows scattered intensity with arrows depicting time average power flow.

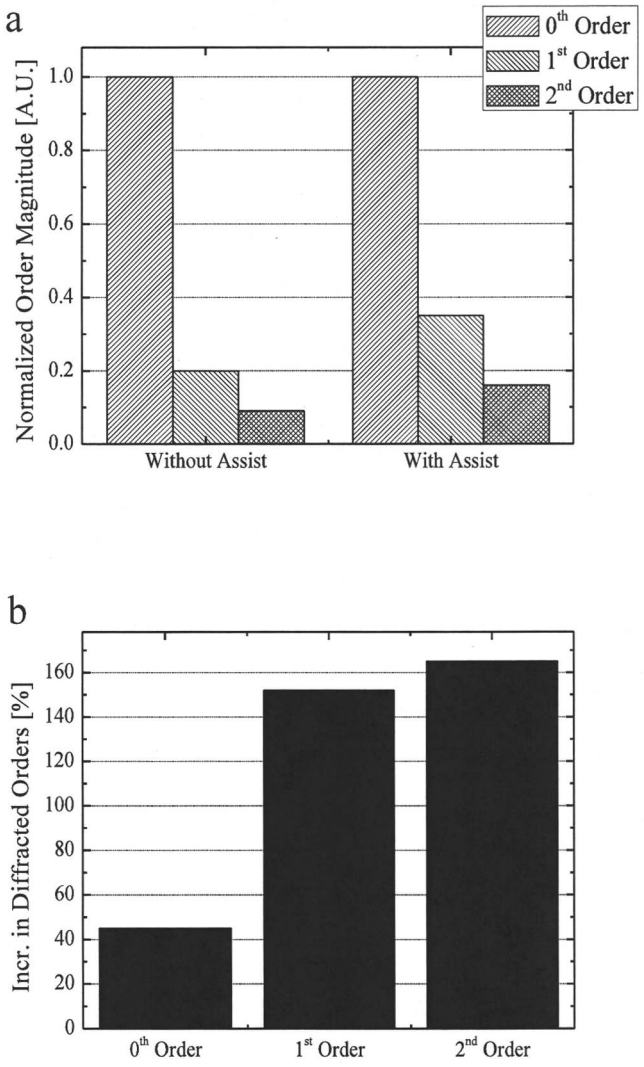

FIG. 6. Diffracted order comparison for the case of $\lambda/CD=3.24$. The simulated wavelength is 730 nm. (a) The magnitude of the electric field of the diffracted orders indicates a relative increase in first and second orders. (b) Comparing the diffracted order electric field magnitudes, zeroth, first, and second orders experience an increase; however, the primary imaging orders experience a larger enhancement, contributing to an improved aerial image.

contrast of the aerial image. To allow for a better comparison, the diffracted order magnitudes are normalized to the zeroth order magnitude, and can be seen in Fig. 6(a). In the unassisted case, the ratio of the diffracted electric field magnitudes for the first and zeroth orders is

$$\frac{|E_1|}{|E_0|} = 0.20, \quad \text{no assist slots},$$

$$\frac{|E_1|}{|E_0|} = 0.35, \quad \text{with assist slots}.$$

The change in zeroth, first, and second orders as assist grooves are added was also analyzed and is shown in Fig. 6(b). Both the first and second orders from the five slot periodic pattern show above a 1.5× increase in scattered order magnitude for this case.

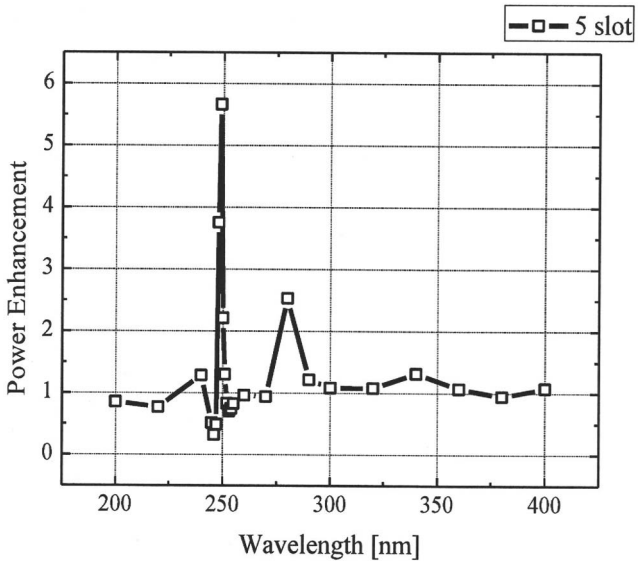

FIG. 7. Power enhancement for the case of aluminum absorber on fused silica substrate. The design is scaled such that maximum power enhancement though the system occurs at 248 nm. The results may also be scaled to 193 nm.

C. Application to deep-UV optical lithography

To demonstrate extension of this technique to a lithographic wavelength, simulations at 248 nm illumination wavelength were performed. On a photomask, the dielectric region above the metal film is replaced with fused silica $n=1.5$, $k=0$.[9] In this case, it is merely a higher index nonabsorbing dielectric. It is also unrealistic to use silver in the deep-UV (DUV) regime, since the metal is not as conductive as in the visible or near-IR ($\mathrm{Re}[\varepsilon]_{\lambda=248}=-0.13$). Aluminum was chosen as the absorber instead since in this region of the spectrum it has excellent optical properties with $\mathrm{Re}[\varepsilon]_{\lambda=248}=-8.73$.[9] The relative size of the simulation domain and geometries for the five assist slot case were scaled to an appropriate size for the 248 nm wavelength. Final dimensions for this case were a transmitting slot with critical dimension (CD) at wafer of 66.5 nm with a pitch of 288 nm at wafer, assist groove width of 30 nm with a depth of 15 nm on a pitch of 192 nm, and an Al thickness of 86 nm. Power enhancement with respect to wavelength may be seen in Fig. 7. Although the region of maximum power enhancement occupies a small portion of the spectrum with very steep slope, the peak was successfully engineered to occur at 248 nm with a value of 5.7. Similar structures should also provide enhancement at 193 nm wavelengths, since the material properties do not change appreciably in that interval.

III. CONCLUSION

Photomask patterns consisting of several different sizes of transmitting apertures surrounded by buried assist grooves have been investigated. For the case of subwavelength apertures, the results seem to agree with previously published data for unpolarized light and conductive films, although the metric for transmission enhancement is different.[2] It has also

been shown that with insulating films suitably patterned on an insulating substrate, a similar type of image enhancement occurs.[4] In that case, the corrugation pattern, polarization, and model differ from those presently described in this work. Further study is needed to establish the exact differences and/or similarities between enhancement mechanisms although their effects are similar.

Also studied was the effect of peripheral grooves on transmission through a larger than wavelength aperture in a metallic film, of special interest for lithographic applications. In this case, the enhancement of power through a free space silver slot has a peak of 1.68× at 730 nm. The peak enhancement region is also slightly redshifted, most likely due to the impact that the large hole in the mask absorber region has on the surface. At peak power enhancement when slot size is larger than the illuminating wavelength, energy is transferred to the primary imaging orders. In the freestanding case with five slots, first and second diffraction order magnitudes improved by factors of 1.52 and 1.65, respectively.

Finally the model was applied to a photomask-type structure at 248 nm illumination wavelength. The profile is very sharp, but also features a best case enhancement of 5.7×, making it the best case studied to date in terms of power enhancement in the DUV region. This type of enhancement scheme could be applied to wafer level features as small as 46 nm at 1:1 duty ratios at the 193 nm illumination wavelength.

ACKNOWLEDGMENTS

The authors gratefully acknowledge the support of Intel and the Semiconductor Research Corporation (SRC).

[1]B. W. Smith and J. R. Sheats, *Microlithography: Science and Technology*, 1st ed. (Dekker, New York, 1998).
[2]H. J. Lezec and T. Thio, Opt. Express **12**, 3629 (2004).
[3]See, for example, A. Nahata and R. A. Linke, Opt. Lett. **28**, 423 (2003).
[4]N. V. Lafferty, J. Zhou, and B. W. Smith, Proceedings of the Microlithography XX, San Jose, edited by D. G. Flagello (SPIE, Bellingham, WA, 2007), p. 652041.
[5]B. W. Smith and D. E. Ewbank, Proceedings of the Microlithography XV, Santa Clara, 2002, edited by A. Yen (unpublished), Vol. 148.
[6]COMSOL Multiphysics v3.3.
[7]S. A. Maier, *Plasmonics: Fundamentals and Applications*, 1st ed. (Springer, New York, 2007).
[8]E. G. Loewen and E. Popov, *Diffraction Gratings and Applications*, 1st ed. (Dekker, New York, 1997).
[9]RIT Center for Nanolithograpy Research, Optical Properties of Thin Films, http://www.rit.edu/lithography.